JASA ARTICLE

Measurement and empirical evaluation of acoustic loss in tube with abrupt area change

Yuki Ueda,[a] Shunsuke Yonemitsu, Kenichiro Ohashi, and Takuya Okamoto
Graduate School of Bio-Applications and Systems Engineering, Tokyo University of Agriculture and Technology, 2-24-16 Nakacho, Koganei, Tokyo 184-8588, Japan

ABSTRACT:
This study measures the acoustic power loss that occurs when an acoustic wave passes through a tube with an abrupt change in area. It is determined that the power loss is proportional to the third power of the velocity amplitude, and that the proportionality coefficient depends upon the area change ratio of the tube. On the other hand, the proportionality coefficient is almost independent of the acoustic impedance and frequency in the 80–250 Hz range. Furthermore, the effect of a tapered tube in reducing the coefficient is experimentally investigated. Based on these experimental results, an empirical estimation method for the acoustic power loss is proposed and validated using a high-pressure-helium-filled tube. © *2020 Acoustical Society of America*. https://doi.org/10.1121/10.0000597

(Received 3 September 2019; revised 9 December 2019; accepted 23 December 2019; published online 29 January 2020)
[Editor: Sean F. Wu] Pages: 364–370

I. INTRODUCTION

When fluids flow in tubes, two types of energy loss occur: One is due to the tube length, whereas the other is due to geometrical irregularities, such as abrupt area change, bifurcation, and bend. The latter is referred to as minor loss.[1–5] For unidirectional fluid flow, both types of losses have been investigated and are well documented in several textbooks on fluid dynamics. However, for oscillatory fluid flow, only few studies[1–5] have addressed the minor loss, although energy loss due to the tube length[7–9] has been well understood.

Wakeland and Keolian[3] showed an equation for the acoustic minor loss. This equation is based on the Bernoulli equation and is expressed as follows:

$$\Delta W = \frac{2}{3\pi}\rho_m S K |U|^3, \tag{1}$$

where ΔW is the acoustic minor loss, ρ_m is the time averaged density of the working gas, S is the cross-sectional area of the tube, where the minor loss occurs, $|U|$ is the peak amplitude of the oscillatory velocity averaged over the cross-sectional area of the tube, and K is the coefficient of the minor loss. Hence, the acoustic minor loss can be estimated if the value of K is known. Because K cannot be theoretically derived, there is a need for empirical determination.

Abrupt area change generated by the connection of two tubes with different cross-sectional areas is one of the most common geometrical irregularities in acoustic systems. Morris *et al.*[4] computationally investigated the acoustic minor loss in a sharp-edged expansion with a tube cross-section-area ratio of 0.01, and presented the flow structure at the vicinity of the expansion point. Based on this result, the minor loss factor was derived. Smith and Swift[2] experimentally investigated the acoustic minor loss with an infinite area ratio and elucidated the effects of a rounded edge at the connecting point. King and Smith, and Doller experimentally investigated the effect of a tapered tube on the minor loss, and showed the minor loss can be reduced by a tapered tube.[5,6]

One of the critical parameters of the abrupt area change is the ratio of the cross-sectional areas of the tubes. However, research on the variation of the area ratio is limited as mentioned above. Hence, we evaluate the effect of the area ratio on the minor loss in this study. The minor loss is measured by changing the velocity amplitude and area ratio. It is confirmed that the minor loss is proportional to the third power of the velocity amplitude, as predicted by Eq. (1). The value of K is experimentally determined as a function of the area ratio. In addition, the effect of the acoustic frequency and acoustic impedance, which depict the oscillatory flow characteristics, is investigated. Furthermore, following King and Smith,[5] and Doller[6] the effect of a tapered tube on the reduction of K is examined. Finally, an empirical equation is introduced for estimating the acoustic minor loss, and validated using a high-pressure-helium-filled tube.

II. EXPERIMENTAL SETUP

The schematic of the experimental apparatus is illustrated in Fig. 1. The apparatus comprises circular tubes A and B connected to each other at a sharp edge, and a unit including a speaker (FW168N, Fostex Co. Ltd.). The cross-sectional areas of tubes A and B are denoted by S_A and S_B, respectively. Tube A is connected to the speaker unit and two pressure sensors (PD-104, JTEKT Co. Ltd.) are mounted on the tube wall. The distance between the sensors is denoted by L_1, and the distance between one of the

[a]Electronic mail: uedayuki@cc.tuat.ac.jp, ORCID: 0000-0002-0284-9927.

https://doi.org/10.1121/10.0000597

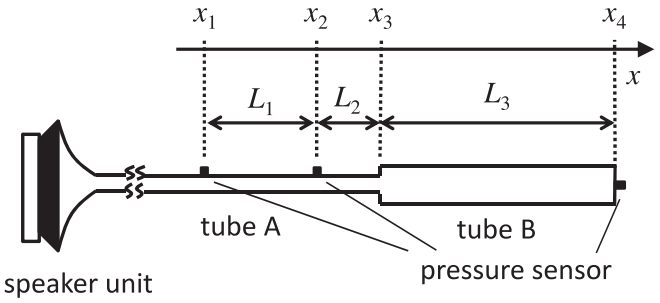

FIG. 1. Schematic of the experimental setup.

sensors and the connecting point (see Fig. 1) is denoted by L_2. One end of tube B is closed by a brass plate on which a pressure sensor (PD-104, JTEKT Co. Ltd.) is mounted. The length of tube B is denoted by L_3. The apparatus is filled with atmospheric air.

In this experiment, the value of $R_{AB} = S_A/S_B$ or its inverse is selected as one of the variable parameters. Table I lists the values of the radius r_A of tube A, radius r_B of tube B, and R_{AB}. Note that the experiments are performed under two conditions, i.e., $R_{AB} \leq 1$ and $R_{AB} > 1$.

III. MEASUREMENT METHOD

As shown in Fig. 1, pressure is measured at two points on the wall of tube A and one point on the closed end of tube B. This section describes the method for evaluating ΔW using the three measured pressure values. This method is similar to the method used in our previous study.[10]

A. Acoustic power and minor loss

It is assumed that an acoustic field with a single frequency is formed in the circular tube, with the x axis set along the length of the tube. The tube radius is assumed to be considerably smaller than the wavelength of the acoustic wave. For expressing the acoustic pressure and cross-sectional mean velocity amplitudes, the complex number $P(x)$ and $U(x)$ are used, respectively. Using $P(x)$ and $U(x)$, the acoustic power, which is the time-averaged rate of acoustic energy transmission through the tube cross-section, is determined as

TABLE I. Radii of tube A (top row) and tube B (left column) and the corresponding R_{AB} values (and $1/R_{AB}$).

r_B(mm) \ r_A(mm)	7.5	12	16	20
7.5	1	2.56 (0.39)	4.55 (0.22)	7.11 (0.14)
12	0.39	1	1.78 (0.56)	2.78 (0.36)
16	0.22	0.56	1	1.56 (0.64)
20	0.14	0.36	0.64	1

$$W(x) = \frac{S}{2}\mathrm{Re}\left[P(x)\tilde{U}(x)\right], \tag{2}$$

where notation $\tilde{}$ indicates the complex conjugate, and S is the cross-sectional area of the tube. If we denote the acoustic power in front and immediately behind the geometrical irregularity by W_+ and W_-, respectively, the acoustic minor loss can be expressed as

$$\Delta W = W^+ - W^-. \tag{3}$$

When acoustic minor loss does not occur, $W_+ = W_-$; hence, $\Delta W = 0$.

B. Theory

Based on the linear acoustic theory, the momentum and continuity equations[12,13] for a circular tube can be expressed as

$$\frac{dP(x)}{dx} = -\frac{i\omega\rho_m}{1-\chi_\upsilon}U(x), \tag{4}$$

$$\frac{dU(x)}{dx} = -\frac{i\omega[1+(\gamma-1)\chi_\alpha]}{\gamma P_m}P(x), \tag{5}$$

where ω is angular frequency, and ρ_m, P_m, γ, and σ are the mean density, mean pressure, specific heat ratio, and Prandtl number of the working gas, respectively. χ_α and χ_ν are complex functions[12–14] that are denoted below. To express these functions, we use two parameters, namely, the thermal relaxation time τ_α and viscous relaxation time τ_ν.[14] These parameters are defined as

$$\tau_\alpha = r^2/(2\alpha), \tag{6a}$$

$$\tau_\nu = r^2/(2\nu), \tag{6b}$$

where r is the tube radius, α is the thermal diffusivity of the working gas, and ν is its kinematic viscosity. For a circular-cross-section tube, functions χ_α and χ_ν are expressed as[12–14]

$$\chi_\alpha = \frac{2J_1(Y_\alpha)}{Y_\alpha J_0(Y_\alpha)}, \tag{7a}$$

$$\chi_\nu = \frac{2J_1(Y_\nu)}{Y_\nu J_0(Y_\nu)}, \tag{7b}$$

where

$$Y_\alpha = (i-1)\sqrt{\omega\tau_\alpha}, \tag{8a}$$

$$Y_\nu = (i-1)\sqrt{\omega\tau_\nu}. \tag{8b}$$

Equations (4) and (5) can be solved analytically. With the obtained solution, the pressure and cross-sectional mean velocity at $x = x_b$ can be expressed by those at $x = x_a$ as[11,15]

$$\begin{pmatrix} P(x_b) \\ U(x_b) \end{pmatrix} = M(x_a, x_b) \begin{pmatrix} P(x_a) \\ U(x_a) \end{pmatrix}$$
$$M(x_a, x_b) \equiv \begin{pmatrix} m_{11}(x_a, x_b) & m_{12}(x_a, x_b) \\ m_{21}(x_a, x_b) & m_{22}(x_a, x_b) \end{pmatrix}$$
$$m_{11}(x_a, x_b) = \cos\left(k(x_b - x_a)\right)$$
$$m_{12}(x_a, x_b) = -iZ_0 \sin\left(k(x_b - x_a)\right)$$
$$m_{21}(x_a, x_b) = \frac{-i}{Z_0} \sin\left(k(x_b - x_a)\right)$$
$$m_{22}(x_a, x_b) = \cos\left(k(x_b - x_a)\right). \quad (9)$$

Here, k is the complex wave number and Z_0 is the characteristic impedance calculated as

$$k = \frac{\omega}{c}\sqrt{\frac{1 + (\gamma - 1)\chi_\alpha}{1 - \chi_\nu}}, \quad (10)$$

and

$$Z_0 = \rho_m \frac{\omega}{k(1 - \chi_\nu)}, \quad (11)$$

respectively, where c is the adiabatic sound speed.

First, let us consider the method for evaluating W^+ using the pressure measured at the two locations on the wall of tube A. The measuring points are set as x_1 and x_2, respectively, and the junction point is set as x_3, as shown in Fig. 1. From Eq. (9),

$$U(x_1) = \frac{P(x_2) - m_{11}(x_1, x_2)P(x_1)}{m_{12}(x_1, x_2)}. \quad (12)$$

Equation (9) is represented as

$$\begin{pmatrix} P(x_3) \\ U(x_3) \end{pmatrix} = M(x_1, x_3) \begin{pmatrix} P(x_1) \\ U(x_1) \end{pmatrix}, \quad (13)$$

and hence,

$$\begin{aligned} \begin{pmatrix} P(x_3) \\ U(x_3) \end{pmatrix} &= M(x_1, x_3) \begin{pmatrix} P(x_1) \\ \dfrac{P(x_2) - m_{11}(x_1, x_2)P(x_1)}{m_{12}(x_1, x_2)} \end{pmatrix} \\ &= M(x_1, x_3) \begin{pmatrix} 1 & 0 \\ \dfrac{-m_{11}(x_1, x_2)}{m_{12}(x_1, x_2)} & \dfrac{1}{m_{12}(x_1, x_2)} \end{pmatrix} \\ &\quad \times \begin{pmatrix} P(x_1) \\ P(x_2) \end{pmatrix}. \end{aligned} \quad (14)$$

Substituting L_1 and $L_2 + L_1$ for $(x_2 - x_1)$ and $(x_3 - x_1)$, respectively, in Eq. (14), we can obtain the pressure P and velocity U at $x = x_3$, i.e., at the junction. With $P(x_3)$, $U(x_3)$, and Eq. (2), the acoustic power W^+ at the connecting point tube A is obtained.

Next, let us consider the method for expressing the acoustic power W^- at the connecting point of tube B. We set the closed end as x_4, and modify Eq. (9) as

$$\begin{pmatrix} P(x_3) \\ U(x_3) \end{pmatrix} = M(x_4, x_3) \begin{pmatrix} P(x_4) \\ U(x_4) \end{pmatrix}. \quad (15)$$

At the closed end, the velocity becomes zero and the pressure P_{closed} is measured. Substituting $x_3 - x_4 = -L_3$, $P(x_4) = P_{closed}$, and $U(x_4) = 0$ in Eq. (15), we can obtain $P(x_3)$ and $U(x_3)$ at the connecting point of tube B. With $P(x_3)$, $U(x_3)$, and Eq. (2), we can calculate W^-. It should be noted that the values of $P(x_3)$ and $U(x_3)$ for calculating W^- are not equal to the values of $P(x_3)$ and $U(x_3)$ for W^+. Substituting the obtained W_+ and W_- in Eq. (3), we can evaluate the acoustic minor loss ΔW.

IV. RESULTS

A. Preliminary experiment

To verify the experimental method described in Sec. III, we perform the experiment with $R_{AB} = 1$. Both r_A and r_B are set to 7.5, 12, 16, and 20 mm, respectively. The lengths L_1 and $L_2 + L_3$ are set to 390 and 750 mm, respectively. The frequency, $\omega/(2\pi)$, of the input acoustic wave is maintained at 161 Hz which is the second resonant frequency of the gas column in the setup. As a result of the use of the second resonance frequency, the velocity antinode appears between x_2 and x_4 rather than in the vicinity of the speaker unit.

Although there is no cross-sectional variation, we set a virtual connecting point at the velocity antinode and measured $W^+ - W^-$; this is denoted by δW. In Fig. 2, the measured δW is depicted as a function of the velocity amplitude $|U|$, where the value of r shown in this figure refers to the radius of the circular tube cross-section. Notably, the maximum $|U|$ for each r shown in Fig. 2 is approximately equal to the maximum $|U|$ obtained by measuring ΔW described in Sec. IV B. As observed in Fig. 2, δW is nonzero and depends upon $|U|$ with $S = r^2\pi$, i.e., $\delta W(U, S)$. The dotted and solid lines in Fig. 2 show functions proportional to $|U|^2$ and $|U|^3$, respectively. They indicate that $\delta W(U, S) \propto |U|^2$ when $|U| < 10$ m/s, whereas $\delta W(U, S) \propto |U|^3$ when $|U| > 20$ m/s. In addition, the repeatability of the measured value of δW was confirmed. We consider that when $|U| < 10$ m/s, the source of $\delta W(U, S)$ is the underestimation of tube wall attenuation due to the viscosity and thermal conductivity of the gas. On the other hand, $|U| > 20$ m/s,

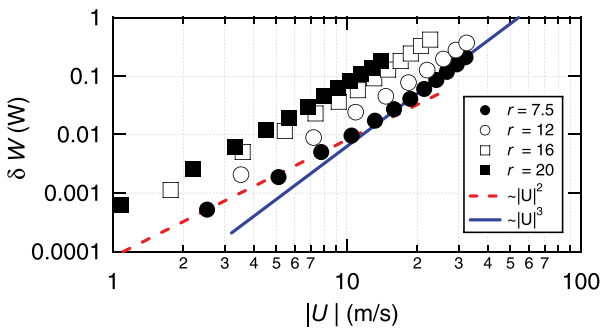

FIG. 2. (Color online) Measured δW in a straight tube as a function of the velocity amplitude at the velocity antinode.

https://doi.org/10.1121/10.0000597

$\delta W(U,S)$ can be attributed to nonlinearity due to the large amplitude of the oscillatory velocity.[16–18] When $|U|$ is maximized for each r, the Reynolds number Re_{os} determined using $|U|$ and $2r$ approaches or just exceeds the critical value[17,18] above which flow becomes turbulent. For example, when $r = 7.5$ mm, the maximum velocity amplitude is 32 m/s, thus, $Re_{os} = 2.7 \times 10^4$, while the critical Re_{os} estimated by the equation proposed by Merkli and Thomann[18] is 2.3×10^4. Based on these preliminary experimental results, we suggest that $\delta W(U,S)$ represents the additional losses occurring in a straight section of the tubes and assume that $\delta W(U,S)$ is proportional to the length of the tube, L. Instead of Eq. (3), we use

$$\Delta W = \left(W^+ - \frac{L_1 + L_2}{L_1 + L_2 + L_3}\delta W(U_A, S_A)\right) - \left(W^- + \frac{L_3}{L_1 + L_2 + L_3}\delta W(U_B, S_B)\right), \tag{16}$$

for measuring ΔW, where U_A and U_B are $U(x_3)$ in tube A and tube B, respectively. Note that the impact of the additional loss on the value of K is found to be approximately 0.15.

B. Measurement of the acoustic minor loss

In this study, we investigate the effect of three factors on the value of K: the effect of the ratio of the tube cross-sectional area R_{AB}, absolute value of the acoustic impedance ($|Z| = |P|/|U|$), and frequency $[\omega/(2\pi)]$.

1. Effect of the tube cross-sectional area ratio on the acoustic minor loss coefficient

In the experimental setup shown in Fig. 1, the pressure and velocity amplitudes depend on position x. To highlight the effect of the velocity amplitude while minimizing the effect of the pressure amplitude, we set the connecting point in the vicinity of the velocity antinode. According to previous research,[19] the velocity amplitude $|U|$ at the connecting point in the narrower tube is used as the representative value.

In Fig. 3, the measured ΔW is depicted as a function of $|U|^3$. The experimental conditions are $\omega/(2\pi) = 161$ Hz, $L_1 = 390$ mm, $L_2 = 250$ mm, $L_3 = 500$ mm, and $R_{AB} = 0.36$ ($r_A = 12$ mm and $r_B = 20$ mm). Figure 3 shows that the value of ΔW linearly increases with the increase in $|U|^3$. When $|U| = 33.4$ m/s ($|U|^3 \sim 37000$ m^3/s^3), ΔW is 2.59 W. This value is considerably greater than the δW for straight tubes. [See data indicated by the unfilled circle at $|U| = 33$ m/s and that indicated by the filled square at $|U| = 12$ m/s ($= 33 \times R_{AB}$ m/s) in Fig. 2.] Hence, we can conclude that acoustic minor loss is generated in the setup.

As previously mentioned, the measured ΔW is proportional to the third power of $|U|$; hence, we can use Eq. (1), as suggested by Swift[13] and Wakeland and Keolian.[3] Using the least squares method, the gradient of g of the obtained data is calculated to be 7.0×10^{-5} kg/m. From Eq. (1), g can be related to the acoustic minor loss coefficient K as follows:

$$K = \frac{3\pi}{2S_i\rho_m}g, \tag{17}$$

where S_i is the cross-sectional area of the narrower tube and $S_i = S_A$ for this case; hence $K = 0.60$ with $R_{AB} = 0.36$.

Next, we perform the experiment with several values of R_{AB} and determine the value of K. The relationship between K and R_{AB} or $1/R_{AB}$ is shown in Fig. 4. The unfilled symbols indicate the data under the expansion condition ($R_{AB} < 1$) whereas the filled ones indicate the data under the contraction condition ($R_{AB} \geq 1$). It is important to note that when $R_{AB} > 1$, $1/R_{AB}$ is considered as the horizontal axis instead of R_{AB}. As shown in Fig. 4, the obtained value of the acoustic minor loss coefficient K decreases with the increase in R_{AB} and $1/R_{AB}$. The observed dependence of K on $1/R_{AB}$ smoothly connects the value of K numerically predicted by Morris *et al.*[4] and that experimentally obtained by Doller;[6] Morris *et al.*[4] reported that when $1/R_{AB} = 0.01$, $K = 0.9$, whereas Doller showed that when $1/R_{AB} = 0.03$, $K = 0.85$. Furthermore, the data indicated by the unfilled and filled symbols approximately agree with each other; the maximum discrepancy is 0.18. This implies that the minor loss coefficient K can be set to be the same for abrupt tube expansion as well as contraction.

Next, the minor loss coefficient of this study (oscillatory flow case) and that of the unidirectional flow case are compared. According to the textbook,[19] when fluid flows unidirectionally in a tube, the minor loss coefficient becomes

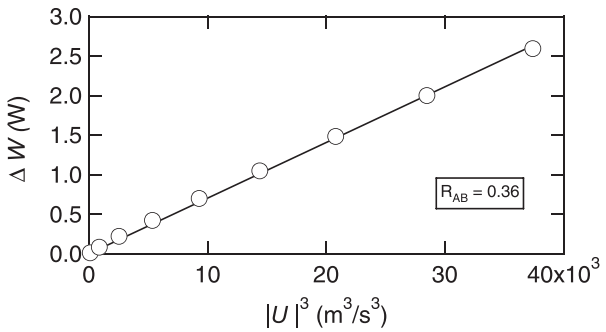

FIG. 3. Measured acoustic minor loss. The radii of tube A and tube B are 12 and 20 mm, respectively, resulting in $R_{AB} = 0.36$.

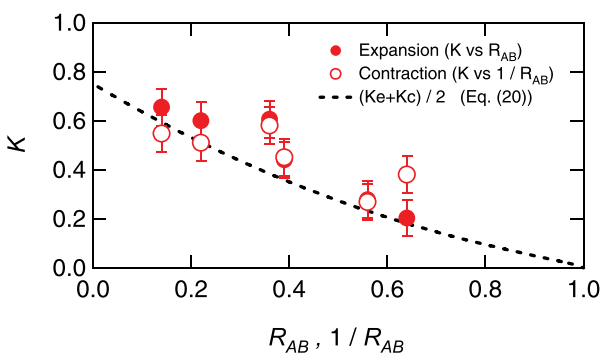

FIG. 4. (Color online) Empirically determined acoustic minor loss coefficient K.

$$K_e = (1 - R_{AB})^2 \quad (R_{AB} < 1) \tag{18}$$

for the expansion condition

$$K_c = 0.5\left(1 - \frac{1}{R_{AB}}\right)^{0.75} \quad (R_{AB} > 1) \tag{19}$$

for the contraction condition. Because the measured result indicates that K is the same in the expansion and contraction cases, we represent the mean of K_e and K_c in Fig. 4 by a dotted line:

$$K = \frac{1}{2}\left(1 - \frac{A_i}{A_j}\right)^2 + \frac{1}{4}\left(1 - \frac{A_i}{A_j}\right)^{0.75} \quad (A_i < A_j). \tag{20}$$

This dotted line shows approximate agreement with the obtained experimental data; hence, Eq. (20) can be used as an approximation for the acoustic minor loss coefficient K.

2. Effect of the acoustic impedance and frequency on the acoustic minor loss coefficient

To investigate the effect of the absolute value of the acoustic impedance on coefficient K, we measure K by varying the connecting point, namely, L_3; The values of L_3 were set to 0.3, 0.4, 0.5, 0.6, and 0.7 m. This implies that the connecting point is located between the pressure and velocity antinodes. In the experiment, R_{AB} is maintained at 0.36 and $\omega/(2\pi)$ is 161 Hz. The measured K is plotted as a function of $|P|/|U|$, as displayed in Fig. 5. The upper limit of $|P|/|U|$ is determined by the performance of the speaker; when $|P|/|U|$ is large, large $|U|$ is not obtained. In Fig. 5, significant dependence of K on the value of $|P|/|U|$ is not obtained. This indicates that the acoustic minor loss is governed by the value of $|U|$, and that the effect of the pressure amplitude $|P|$ on K is less.

Further, we examine the effect of the frequency, $\omega/(2\pi)$, on the value of K. For a fixed value of R_{AB} (= 0.36), K is measured when the frequency of the acoustic wave is varied from 83 to 253 Hz. For this experiment, the length L_3 of tube B is changed such that the connecting point is always fixed in the vicinity of the velocity antinode. The tested values of L_3 were 0.3, 0.4, 0.5, 0.6, 0.8, and 1.0 m. The results (Fig. 6) indicate that the frequency has no significant effect on the value of K in the used frequency range.

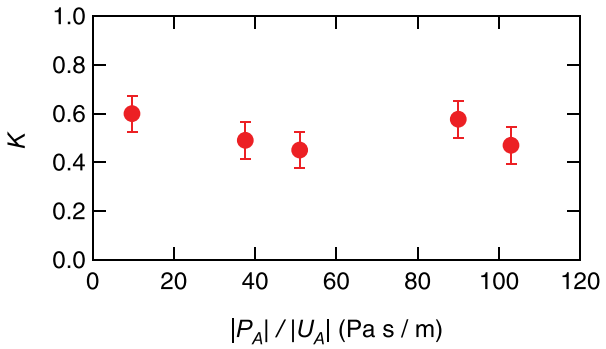

FIG. 5. (Color online) Acoustic impedance dependence of the minor loss coefficient.

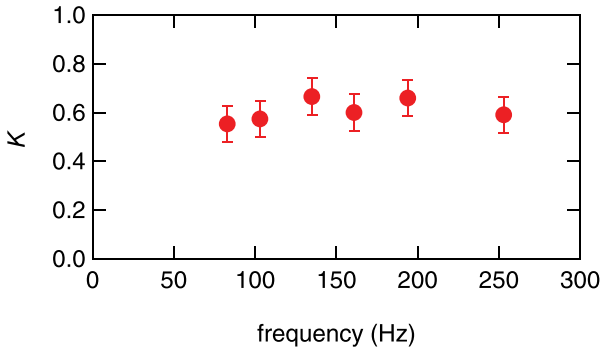

FIG. 6. (Color online) Frequency dependence of the minor loss coefficient.

C. Effect of tapered tube on the minor-loss reduction

To reduce minor loss, a tapered tube with a gradually changing cross-sectional area is generally employed.[1,5,6,20–22] In this section, we demonstrate the quantitative effect of a tapered tube on the reduction of the acoustic minor loss coefficient. As a parameter depicting the tapered tube characteristics, we define the taper angle θ, as shown in Fig. 7. The radii of tubes A and B are fixed at 12 and 20 mm, respectively. The frequency of the input acoustic wave is fixed at 161 Hz, and the tapered tube is positioned in the vicinity of the velocity antinode.

In Fig. 8(a), the evaluated K is depicted as a function of θ. The condition $\theta = 90°$ refers to an abrupt area change, whereas $\theta = 0°$ indicates a straight tube. Note that in this evaluation, the effect of the dissipation due to the length of the tapered tube is included in K; hence, K will become infinity when $\theta = 0°$. However, when $\theta = 8°$, the length of the tapered tube is 56 mm and the effect of the dissipation due to the length is negligible in the conducted experiments. As observed in Fig. 8(a), when $\theta > 15°$, the minor loss coefficient K reduces with the decrease in θ, and the value of K at $\theta = 30°$ becomes less than half of that without the tapered tube. Note that the lengths of the tapered tube at $\theta = 60°$ and 30° are 4.6 and 14 mm, respectively, and are comparable to the radii of the tubes. Furthermore, the value of K at $\theta = 15°$ is almost equal to that of a straight tube within the error margin. Therefore, we can conclude that the use of a

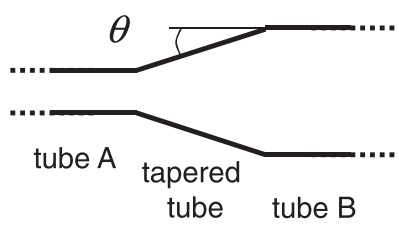

FIG. 7. Schematic of the used tapered tube and the definition of the taper angle θ.

https://doi.org/10.1121/10.0000597

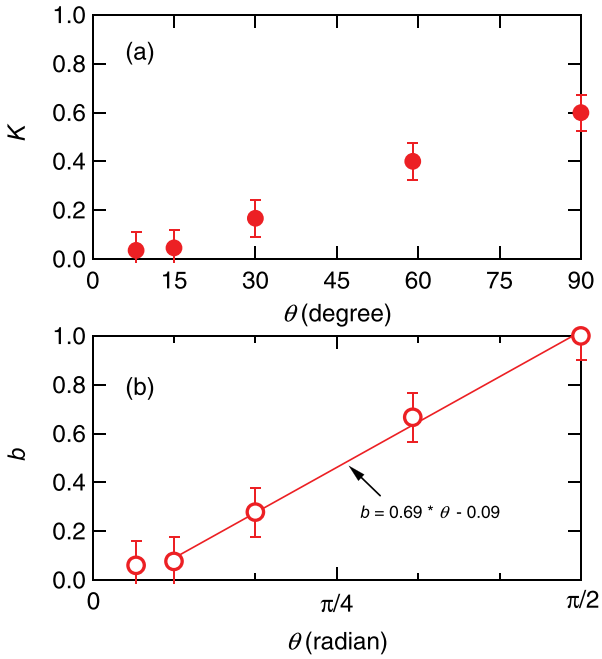

FIG. 8. (Color online) The taper angle dependence of the (a) minor loss coefficient and (b) normalized coefficient $b = K/K_{\theta=\pi/2}$.

tapered tube is an effective method for reducing the acoustic minor loss, and that a tapered tube with a length comparable to the tube radius can reduce the acoustic minor loss by half.

To obtain the approximation of the effect of the taper angle, we introduce the normalized coefficient $b = K/K_{\theta=\pi/2}$ and plot it in Fig. 8(b). As observed in this figure, when $\pi/2 > \theta > \pi/12$, b is almost a linear function of θ and can be approximately expressed as

$$b(\theta) = 0.69 \times \theta - 0.09. \tag{21}$$

Therefore, we propose an empirical equation to estimate the acoustic minor loss for coupling Eqs. (20) and (21) as follows:

$$K = b(\theta) \times \left(\frac{1}{2}\left(1 - \frac{A_i}{A_j}\right)^2 + \frac{1}{4}\left(1 - \frac{A_i}{A_j}\right)^{0.75}\right)$$
$$(A_i < A_j, \pi/12 < \theta < \pi/2). \tag{22}$$

V. VALIDATION OF THE OBTAINED EMPIRICAL *K*

In order to validate Eq. (22), we perform an experiment using pressurized helium as a working fluid. The experimental setup is composed of a power source (thermoacoustic engine), resonator, and tank, as shown in Fig. 9. The setup is filled with helium at a time-averaged pressure of 0.8 or 1.1 MPa. The inner radii the neck tube and the tank are 49 and 195 mm, respectively, (Fig. 9); hence, ratio $A_i/A_j = 0.063$. The taper angle θ is estimated using CAD data and is 33°. Note that because welding is used to connect the neck tube to the tapered tube, the connecting point is not sharp. Substituting these values in Eqs. (21) and (22), we obtain $K = 0.21$.

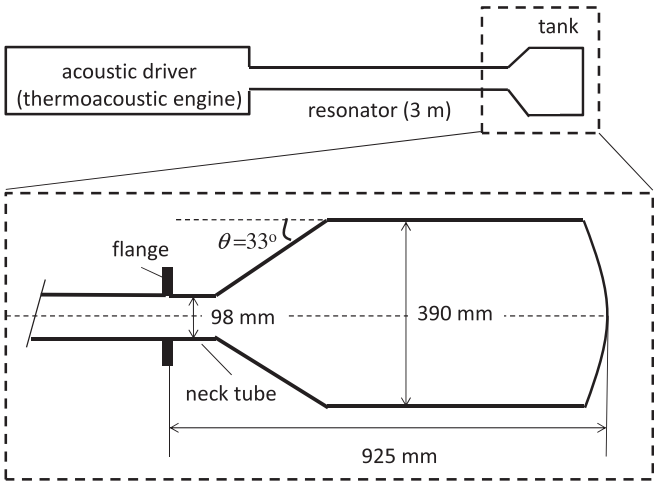

FIG. 9. Schematic illustration of the experimental setup for validation.

Pressure sensors are mounted on the wall of the resonator and the acoustic power flowing to the tank is measured when the velocity amplitude is varied. All this acoustic power is dissipated in the tank mainly at the point where the cross-section changes. The power source generates an acoustic wave of 59 ± 1 Hz, and the velocity antinode is found to be located near the tank inlet.

The measured acoustic power with 0.8 MPa helium and that with 1.1 MPa helium, respectively, are depicted by unfilled and filled squares in Fig. 10 as a function of the cubic of the velocity amplitude, respectively. The dissipated power is approximately proportional to the cubic of $|U|$ and the time averaged pressure, as expected based on Eq. (1). Using $K = 0.21$ and Eq. (1), we estimate the minor loss, and display it in Fig. 10 using solid and dotted lines. In this figure, the estimated loss is in good agreement with the measured power. Therefore, we conclude that Eq. (22) can be used for estimating the acoustic minor loss.

VI. CONCLUSION

In this study, the minor loss that occurs at abrupt changes in the tube cross-section was measured, and the minor loss coefficient K was experimentally determined. It was established that K is independent of the frequency and acoustic impedance, and that the dependence of K on the

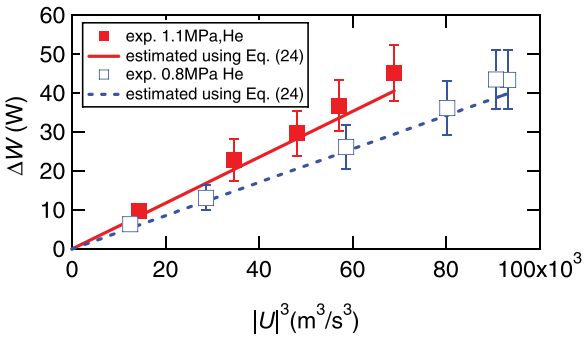

FIG. 10. (Color online) Measured acoustic power and estimated minor loss.

cross-sectional area ratio can be expressed by an equation based on the minor loss coefficient for unidirectional flow. Furthermore, the reduction effect of a tapered tube on K was investigated. When the taper angle $\theta = 15^\circ$, K was reduced to 10% of that without the tapered tube. An empirical model was proposed based on the obtained data, in addition. The proposed model was validated using a system filled with pressurized helium; the estimated and experimental data were in good agreement.

ACKNOWLEDGMENTS

This work was supported by JSPS KAKENHI Grant No. 19H02607.

[1]A. Petculescu and L. Wilen, "Oscillatory flow in jet pumps: Nonlinear effects and minor losses," J. Acoust. Soc. Am. **113**, 1282–1292 (2003).
[2]B. Smith and G. W. Swift, "Power dissipation and time-averaged pressure in oscillating flow through a sudden area change," J. Acoust. Soc. Am. **113**, 2455–2463 (2003).
[3]R. S. Wakeland and R. M. Keolian, "Influence of velocity profile nonuniformity on minor losses for flow existing thermoacoustic heat exchangers," J. Acoust. Soc. Am. **115**, 2071–2074 (2004).
[4]P. J. Morris, S. Boluriaan, and C. M. Shieh, "Numerical simulation of minor losses due to a sudden contraction and expansion in high amplitude acoustic resonators," Acta Acust. Acust. **90**, 393–409 (2004), see https://www.ingentaconnect.com/content/dav/aaua/2004/00000090/00000003/art00002.
[5]C. V. King and B. L. Smith, "Oscillating flow in a 2-d diffuser," Exp. Fluids **51**, 1577–1590 (2011).
[6]A. J. Doller, "Acoustic minor losses in high amplitude resonators with single-sided junctions," Ph. D. dissertation, Pennsylvania State University, 2004.
[7]H. Tijdeman, "On the propagation of sound waves in cylindrical tubes," J. Sound Vib. **39**, 1–33 (1975).
[8]T. Yazaki, Y. Tashiro, and T. Biwa, "Measurements of sound propagation in narrow tubes," Proc. R. Soc. London, Ser. A **463**, 2855–2862 (2007).
[9]T. Biwa, Y. Tashiro, H. Nomura, Y. Ueda, and T. Yazaki, "Experimental verification of a two-sensor acoustic intensity measurement in lossy ducts," J. Acoust. Soc. Am. **124**, 1584–1590 (2007).
[10]Y. Ueda and N. Ogura, "Measurement of acoustic dissipation occurring in narrow channels with wet wall," J. Acoust. Soc. Am. **145**, 71–76 (2019).
[11]D. Mapes-Riordan, "Horn modeling with conical and cylindrical transmission-line elements," J. Audio. Eng. Soc. **41**, 471–484 (1993).
[12]N. Rott, "Damped and thermally driven acoustic oscillations," Z. Angew. Math. Phys. **20**, 230–243 (1969).
[13]G. W. Swift, *Thermoacoustics: A Unifying Perspective for Some Engines and Refrigerators* (Acoustical Society of America, Pennsylvania, 2002).
[14]A. Tominaga, *Fundamental Thermoacoustics* (Uchidarokakumo, Tokyo, 1998).
[15]Y. Ueda and C. Kato, "Stability analysis for spontaneous gas oscillations thermally induced in straight and looped tubes," J. Acoust. Soc. Am. **124**, 851–858 (2008).
[16]T. Biwa and T. Yazaki, "Observation of energy cascade creating periodic shock waves in a resonator," J. Acoust. Soc. Am. **127**, 1189–1192 (2010).
[17]M. Ohmi and M. Iguchi, "Critical Reynolds number in an oscillating pipe flow," Bull. JSME **25**, 165–172 (1982).
[18]P. Merkli and H. Thomann, "Transition to turbulence in oscillation pipe flow," J. Fluid Mech. **68**, 567–575 (1975).
[19]I. Idelchik, *Handbook of Hydraulic Resistance* (Jaico, Munbai, 2003).
[20]S. Backhaus and G. W. Swift, "A thermoacoustic Stirling engine," Nature **399**, 335–338 (1999).
[21]J. P. Oosterhuis, S. Buhler, D. Wilcox, and T. H. Van der Meer, "A numerical investigation on the vortex formation and flo separation of the oscillatory flow in jet pumps," J. Acoust. Soc. Am. **137**, 1722–731 (2015).
[22]J. P. Oosterhuis, S. Buhler, D. Wilcox, and T. H. Van der Meer, "Jet pumps for thermoacoustic applications: Design guidelines based on a numerical parameter study," J. Acoust. Soc. Am. **138**, 1991–2002 (2015).